

Solvation Free Energy Profile of the SCN⁻ Ion Across the Water - 1,2-Dichloroethane Liquid/Liquid Interface. A Computer Simulation Study

Mária Darvas,^{1,2,*} Miguel Jorge³, M. Natalia D. S. Cordeiro⁴, and Pál Jedlovszky^{1,5,6},

¹*Laboratory of Interfaces and Nanosize Systems, Institute of Chemistry, Eötvös Loránd University, Pázmány P. Szny 1/A, H-1117 Budapest, Hungary*

²*Institut UTINAM—UMR CNRS 6213, Faculté des Sciences, Université de Franche-Comté, F-25030 Besançon Cedex, France*

³*LSRE/LCM - Laboratory of Separation and Reaction Engineering, Faculdade de Engenharia da Universidade do Porto, Rua Dr. Roberto Frias, 4200-465 Porto, Portugal*

⁴*REQUIMTE, Faculdade de Ciências da Universidade do Porto, Rua do Campo Alegre, 687, 4169-007 Porto, Portugal*

⁵*HAS Research Group of Technical Analytical Chemistry, Szt. Gellért tér 4, H-1111 Budapest, Hungary*

⁶*EKF Department of Chemistry, Leányka utca 6, H-3300 Eger, Hungary*

Running title: Free energy profile of SCN⁻ across the water-DCE interface

*Electronic mail: maria.darvas@univ-fcomte.fr

Abstract:

The solvation free energy profile of a single SCN^- ion is calculated across the water - 1,2-dichloroethane liquid/liquid interface at 298 K by the Constraint Force method. The obtained results show that the free energy cost of transferring the ion from the aqueous to the organic phase is about 70 kJ/mol. The free energy profile shows a small but clear well at the aqueous side of the interface, in the subsurface region of the water phase, indicating the ability of the SCN^- ion of being adsorbed at a close vicinity to the interface. Upon entering the SCN^- ion to the organic phase a co-extraction of the water molecules of its first hydration shell occurs. Accordingly, when it is located at the boundary of the two phases the SCN^- ion prefers orientations in which its bulky S atom is located at the aqueous side, and the small N atom, together with its first hydration shell, at the organic side of the interface.

1. Introduction

It is a widely-known fact supported by data obtained from classical surface tension measurements that the interfacial tension increases upon addition of inorganic salts to their aqueous solutions.¹⁻⁵ The first explanation of this phenomenon by Onsager and Samaras⁶ was based on describing the ion as a simple point charge and the interface as a sharp and flat discontinuity between two continuous media of remarkably different dielectric permittivity. In the framework of this theory, the repulsion of ions from the interface is expected as a result of the force exerted on them by the image charge formed in the opposite phase.⁷ This pioneering theory has been further developed and elaborated by the addition of surface effects to the original model.^{3,8-15} However, all the presently existing versions of the original theory predict a monotonically decreasing distribution of ions upon approaching the interface along the surface normal axis, and eventually claim the existence of an ion free region situated right at the surface. Experiments carried out with advanced surface analyzing methods, such as sum frequency generation (SFG) and second harmonic generation (SHG) spectroscopy, and with highly developed electrochemical techniques for both liquid/vapor¹⁶⁻¹⁹ and liquid/liquid interfaces,²⁰⁻²⁴ disproved the general validity of the above described theory by detecting the enhancement of the ion concentration at the surface region for certain ions. These findings seemingly contradict the results of surface tension measurements, but considering the fact that these novel methods target solely the outermost surface layer of the systems while the classical surface tension measurements naturally involve the entire system, this contradiction is far from being sharp and evident.

Computer simulation techniques, such as molecular dynamics or Monte Carlo are handy tools to provide us with an in-depth molecular level picture of our systems of interest. Bearing such advantages, these methods have recently been widely used to investigate the behavior of different ions both at the liquid/vapor interface of their solutions²⁵⁻³¹ and at liquid/liquid interfaces formed by the aqueous ionic solution and various organic compounds immiscible with the aqueous phase.³¹⁻⁴¹ Some of these computational studies address directly the question of ionic distribution in the interface normal direction by placing a number of ions into the aqueous phase and calculating their density distribution from the resulting trajectory.³⁸ Such studies showed that only the compact monoatomic ions characterized by low polarizability (e.g., F⁻) obey the original theory of Onsager and Samaras.⁶ The calculated density distributions of such ions show that the interfacial region is in fact depleted to such an extent that leads to the eventual formation of an ion free region, and the monotonous increase

of the ion concentration along the surface normal axis is also observable. Similar studies have been carried out for larger and more polarizable monoatomic ions, like I⁻.^{29,34} Contrary to what has been observed for compact ions such as F⁻, these species were shown to have a tendency to exhibit a density peak directly at the interface followed by a depletion region ranging towards the subsurface layers. This finding sheds light on the apparently positive surface activity of these ions. In their pioneering work Jungwirth and Tobias showed this behavior primarily for the iodide ion, which, in spite of its well-known tendency to increase the surface tension of aqueous solutions, was found to be adsorbed positively in the surface region of its solutions.²⁶ This study was followed by several other simulation studies concerning small polyatomic ions such as SCN⁻, OH⁻ or picrate, all of which are known to be negatively surface active, to shed light on the complex adsorption behavior of these species.³⁶

The other group of computer simulation studies focuses mainly on calculating the solvation free energy profile of ions through various interfaces.³³ A considerable number of such studies have been dedicated to monoatomic anions, such as chloride or iodide, and cations, such as sodium or potassium.²⁹⁻³⁵ To the best of our knowledge, however, there has been only a few works published so far about the calculation of the solvation free energy change accompanying the transfer of a polyatomic ion, namely tetramethylammonium, through the liquid/liquid interface,^{35,42} even if such ions may have considerable importance in nanotechnology,⁴³ organic⁴⁴ and organometallic syntheses,⁴⁵ as well as in atmospheric phenomena or electrochemical industry.

Thiocyanate (SCN⁻) is one of the most widely investigated examples of polyatomic anions. It plays a considerable role in essential biochemical processes, such as the biosynthesis of hypothyroidism, the lack of which is proven to cause cystic fibrosis.⁴⁶ On the other hand, detailed studies of this ion by means of electrochemical experimental techniques (chronoamperometry as well as cyclic voltammetry) date back to the middle of the last century.⁴⁷ Since that time, this ion has attracted an ever increasing interest. Thus, the understanding of the structural and the thermodynamic changes that accompany the transfer of the SCN⁻ ion through a water/organic phase boundary is undoubtedly of crucial interest.

In this study we present a computer simulation calculation of the solvation free energy profile of a single thiocyanate ion across the water-1,2-dichloroethane (DCE) liquid/liquid interface. The choice of DCE as the organic phase is dictated by the fact that the water/DCE system is one of the most widely studied liquid-liquid interfaces, both experimentally⁴⁸⁻⁵³ and by computer simulation methods.^{31,32,37,38,53-60} The transport of various ions across this

interface has also been studied a number of times.^{31,32,38,56} We also address the structural changes invoked in the interface by the presence of the ion.

2. Computational Details

2.1. Equilibration of the Interfacial System. Molecular dynamics simulations of the water-DCE liquid/liquid interfacial system containing one single thiocyanate (SCN^-) ion at different positions have been performed on the canonical (N, V, T) ensemble at 298 K using the GROMACS simulation program package.⁶¹ The lengths of the X , Y and Z edges of the rectangular basic simulation box (X being perpendicular to the macroscopic plane of the interface) have been 104, 50 and 50 Å respectively, and the system consisted of 4000 water and 1014 DCE molecules.

Water molecules have been described by the TIP4P model,⁶² whereas standard OPLS potential parameters⁶³ have been used for the SCN^- ion and for the DCE molecules. The fractional charges corresponding to the DCE molecule have been taken from the pioneering work of Benjamin.⁵⁴ All bond lengths and bond angles have been kept fixed in the simulations, while torsional rotation of the DCE molecule around its C-C bond has been allowed. The force constant k_ϕ and equilibrium angle ϕ_0 of this torsional rotation have been 5.860 kJ/mol and 180° , respectively. The CH_2 groups of the DCE molecules have been treated as united atoms. The total potential energy of the systems has been assumed to be the sum of the pair interaction energies of all molecule pairs. The interaction energy of two molecules has been calculated as the sum of the Lennard-Jones interactions acting between their atoms and of the Coulomb interactions acting between their fractional charges. The Lennard-Jones distance and energy parameters (σ and ε , respectively) of the interacting atoms have been combined according to the Lorentz-Berthelot rule.⁶⁴ The Lennard-Jones parameters as well as the fractional charges, q , of the different interaction sites are collected in Table 1, whereas the bond lengths and bond angles of the molecular models used are summarized in Table 2. Bond lengths and bond angles of the water molecules; and those of the DCE molecules and SCN^- ion have been kept unchanged by means of the SETTLE⁶⁵ and LINCS⁶⁶ algorithms, respectively. All interactions have been truncated to zero beyond the centre-centre cut-off distance of 9.0 Å. The long range part of the electrostatic interaction has been accounted for using the particle mesh Ewald (PME) method⁶⁷ with a real space cutoff of 9.0 Å, a mesh grid of 1.2 Å and a spline order of 4. Analytical tail correction has been applied. To maintain electroneutrality of the system simulated, a uniform positive charge distribution compensating

the net charge of the SCN^- ion has been added beyond the cut-off sphere of the SCN^- ion, and its effect has also been accounted for by means of the PME method. To test the appropriateness of the cut-off value of 9.0 Å used here, we have repeated six simulations with different positions of the SCN^- ion, corresponding to different regions of the system, using a considerably larger interaction cut-off value, i.e., 12.0 Å, but, besides the statistical noise, no difference between the runs performed with different cut-off values has been observed.

The creation and equilibration of the DCE-water interfacial system in the absence of the SCN^- ion has been described in our previous publication,⁶⁰ thus, here we refrain from repeating the detailed description. When setting up the first system containing the ion, a randomly chosen water molecule of the original water/DCE interfacial system, being well inside the bulk aqueous phase, has been replaced by the SCN^- ion. After proper energy minimization this system has been allowed to relax for 1 ns with a simulation time step of 1 fs. Finally, in order to calculate the solvation free energy of the SCN^- ion at various positions along the interface normal axis X , a set of simulations with the ion at various depths along this axis had to be performed. To create the starting configuration of each of these consecutive runs, the SCN^- ion was moved towards the bulk organic phase by 0.5 Å from its final position in the previous run.

2.2. Potential of Mean Force Calculation. The solvation free energy profile of the SCN^- ion, $A(X)$, has been calculated by the Constraint Force method.⁶⁸ To accomplish this, the SCN^- ion has been moved gradually, during the course of the set of simulations, in small equilibrium steps along a path parallel to the interface normal axis from the bulk aqueous to the bulk organic phase, and the time average of the force needed to keep the position of the ion unchanged, F_x , has been recorded for each position. The solvation free energy A of the SCN^- ion at a certain position along the interface normal axis X can finally be obtained as the integral of F_x calculated between the middle of the bulk aqueous phase and the corresponding X value.

In practice, a number of simulations with the thiocyanate ion located at different positions has been performed on the canonical (N, V, T) ensemble in the same way as described in the previous section, with the exception that in each simulation the position of the SCN^- ion along the interface normal axis X has been fixed by means of a constraining force exerted on it.⁵⁵ Following proper energy minimization of the starting configuration and a 100 ps long equilibration with the constraining force exerted on the ion, the magnitude of the X component of the constraining force, $F_x(t)$, has been recorded in every time step of each of

these simulations along a 500 ps long trajectory. This way, for each position of the ion along the interface normal axis X the time average of the force, F_x , could be obtained by simply averaging the force over all the steps.

3. Results and Discussion

3. 1. Solvation Free Energy Profile. The solvation free energy profile of the SCN^- ion obtained from the simulations is shown in Figure 1. Error bars have been estimated by the method of block averages.⁶⁴ For reference, the mass density profile of water and DCE are also indicated. The shape of the obtained profile indicates that the energetic changes accompanying the transfer of the SCN^- ion from the aqueous to the organic phase follow a complex scheme. Thus, on approaching the interface from the bulk aqueous phase a slight increase of the free energy, culminating in a local maximum is seen. Since the solvation free energy of SCN^- inside a bulk liquid phase has to be position independent, this slight increase, typically seen in free energy profile calculations of various ions,⁶⁹ is clearly an artifact, related to the presence of two phases of markedly different dielectric constant under periodic boundary conditions. Clearly, if the ion is embedded to one of the bulk phases, it experiences being in a slit of different dielectric constant than the environment behind the slit. The presence of the two dielectric boundaries results in a (non-physical) net force on the ion, which decreases upon approaching the middle of the phase (where the difference of the distance from the two boundaries becomes smaller), and vanishes only in the middle of the phase, i.e., at equal distance from the two boundaries. The presence of this artificial force results in the slight, albeit noticeable, non-physical decrease of the free energy profile in the bulk aqueous phase.

More importantly, the free energy profile shows a small but clear minimum in the subsurface region of water, around the X value of 15 Å. The ITIM analysis⁷⁰ performed on the ion free system⁶⁰ has revealed that this slight local minimum is located roughly at the position of the fourth molecular layer of water. Interestingly, the furthestmost point to which the DCE molecules can penetrate into the aqueous phase coincides with the outer end of the region where the free energy minimum is observed. This suggests that, presumably due to the presence of the organic molecules, the region where the two phases are in direct contact with each other (i.e., the position of the interface itself) is a thermodynamically less favorable environment for the SCN^- ion than the subsurface water layer. Further, the minimum in the free energy profile indicates enhanced ion concentration just beneath the interface, slightly

pushed back from there to the bulk aqueous phase by the presence of the opposite phase. Similar behavior has been observed both experimentally^{18,71} and by computer simulation methods^{39,69,72} for the free surface of several ionic solutions, with the difference that in these cases the enhanced concentration region was located right at the interface.

The free energy minimum region in the subsurface water layer is followed by a strictly monotonically increasing part of the free energy profile, reflecting the fact that the SCN^- ion stays preferentially in the aqueous rather than in the organic phase. The free energy range covered by this increase (i.e., the solvation free energy difference of the SCN^- ion between the two phases) is found to be roughly 70 kJ/mol. The interfacial increase of the profile is followed by another plateau in the subsurface region of the DCE phase. According to ITIM analysis results of the ion-free system,⁶⁰ the position of this plateau region again coincides roughly with that of the fourth molecular layer beneath the surface. Finally, the profile shows a slightly increasing part in the bulk DCE phase, the slope of this increase being noticeably smaller than that in the bulk aqueous phase, in accordance with the considerably lower polarity of DCE relative to water.

It should finally be noted that the plateau region of the profile in the subsurface DCE phase, contrary to that in water, is located clearly beyond the point up to which the molecules of the other phase can penetrate under equilibrium conditions (i.e., in the lack of a penetrating ion). In other words, the region of the steep free energy increase at the interface ranges beyond the point of noticeable water density further into the bulk organic phase, where finally it reaches its plateau. This behavior can be explained by the possible formation of a water finger around the SCN^- ion when it penetrates into the organic phase, and by the eventual co-extraction of at least a part of the ion's first hydration shell. This well-known phenomenon, observed also in a number of studies^{33-35,69,73} has, to our knowledge, scarcely been quantified by theoretical methods.³⁵

3.2. Properties of the SCN^- Ion in Different Environments. To characterize the hydration and orientation of the SCN^- ion in different environments we have divided the system into six separate regions according to the behavior of the obtained free energy profile. Thus, the bulk water and DCE regions correspond to the slightly rising parts of the profile inside the corresponding phases, subsurface water and DCE regions cover the X ranges of the corresponding plateaus, whilst the interfacial water and DCE regions are located at the position of the steeply rising part of the free energy profile. The boundary between these two latter regions is defined by the X value where the mass density profiles of the two

components, normalized by the corresponding average bulk liquid phase densities, are equal to each other. The division of the system into these six separate regions is demonstrated in Figure 1.

3.2.1. Hydration Properties. To investigate the hydration of the SCN^- ion we have calculated the pair correlation functions of all the three atoms constituting the ion with the water oxygen atoms in the six separate regions of the system. The $g(r)$ functions obtained in the two bulk and interfacial regions are shown in Figure 2. (The pair correlation functions obtained in the two subsurface regions did not differ considerably from those in the respective bulk regions, and hence they are omitted from the figure.) As is seen, the obtained ion-water $g(r)$ functions preserve their main features observed in the bulk aqueous phase, irrespective of which region the ion is situated in. In particular, the height and position of the first peak seems to be insensitive to the region where the ion is located in every case. This finding suggests that the SCN^- ion indeed retains at least its first hydration shell upon entering to the DCE phase.

Having calculated these $g(r)$ functions we can obtain a rough, semi-quantitative estimate of the hydration number of the SCN^- ion, N_{hyd} , by simply adding up the partial hydration numbers n_{hyd} of the S and the N atoms, the latter being the coordination number of the water oxygens around the given atom up to the first minimum position of the corresponding $g(r)$ function (being 3.6 Å and 3.4 Å for S-O and N-O pairs). The partial hydration number of the central C atom (calculated up to the first minimum position of the corresponding $g(r)$ function at 5.5 Å) is disregarded in this estimate because the vast majority of the water molecules being in contact with the central C atom are likely to be in contact also with either the N or the S atom, and hence they are already counted. We are aware of the fact that this approximation might introduce some error in our estimates; however, it seems reasonable to assume that the magnitude of this error is roughly the same in every case. To get some further confidence in our qualitative results, we have also repeated the calculations by including also the partial hydration number of the C atom in N_{hyd} (data not shown). The results obtained this way did not show any qualitative difference with the results presented here.

The hydration numbers calculated this way in the different regions of the system as well as the contributions of the S and N atoms to N_{hyd} are shown in Figure 3, and all the n_{hyd} and N_{hyd} values are also collected in Table 3. Figure 3 indicates that at the vicinity of the interface, regardless of which side of it the ion is situated, the total hydration number decreases noticeably relative to the values obtained in the bulk and subsurface aqueous

regions, however, it gradually retains this value as the ion approaches the bulk DCE phase. Upon approaching the interfacial regions we encounter the decrease of all atomic contributions. It is also seen that the dehydration of the three atoms occurs parallel with each other. Thus, after a smooth decrease all atomic hydration numbers assume a minimal value in the interfacial region of the organic phase. This slight rearrangement of the hydration shell at the interface suggests that the vicinity of the interface (and hence that of a phase of markedly different polarity) probably has an effect of enforcing a preferential orientation on the SCN^- ion.

3.2.2. Orientation. To further investigate this point we have calculated the cosine distribution of the angle γ , formed by the vector pointing along the SCN^- ion from its S to N atom and the interface normal vector pointing from the organic to the aqueous phase, \underline{X} , in the six separate regions of the system. The obtained cosine distributions together with a chart illustrating the definition of the angle γ are shown in Figure 4.

As is expected, no clear orientational preference of the ion is seen in any of the two bulk liquid phases. Upon approaching the DCE phase the SCN^- ion adopts a preferred alignment in which it points with the N atom to the organic and with the S atom to the aqueous phase. In the subsurface water region this preferred orientation is rather strongly tilted, it declines from the plane of the interface by only about 10° . However, as the ion gets closer to the DCE phase its preferred orientation becomes gradually less tilted, and eventually in the subsurface DCE region it becomes perpendicular to the interface, as seen from the gradual shift of the peak of the $P(\cos\gamma)$ distribution down to -1. Obviously, this orientational preference is not preserved when the ion penetrates into the bulk region of the DCE phase.

The observed orientational preferences are related to the considerably larger size of the S than of the N atom. Namely, when the SCN^- ion is located at the boundary of the two phases the free energy cost of bringing the first hydration shell water molecules of the small N atom to the organic side of the interface is clearly smaller than that of the large S atom. Further, the gradual decrease of the tilt angle of the preferred orientation is also related to the fact that the water molecules hydrating the large S atom remain at the aqueous side of the interface until the entire ion (together with its first hydration shell) is completely immersed in the DCE phase. The above interfacial orientational preferences of the SCN^- ion as well as the observed co-extraction of its first hydration shell are illustrated in Figure 5, showing two instantaneous snapshots taken out from the simulations in which the position of the SCN^- ion was fixed close to the boundary of the two phases.

4. Summary and Conclusions

In this paper we have presented detailed calculations for determining the solvation free energy profile of a SCN^- ion across the water-DCE liquid/liquid interface. Our results showed that the free energy cost of transferring the ion from the bulk aqueous to the bulk DCE phase is about 70 kJ/mol. A local free energy minimum has been observed in the subsurface water region, just beyond the point up to which DCE can penetrate into the aqueous phase along the molecularly rugged interface. The presence of this free energy well indicates the ability of the SCN^- ion for being adsorbed at the close vicinity of the interface.

It has also been seen that the SCN^- ion enters into the organic phase along with the water molecules constituting its first hydration shell. This fact also leads to the preference of such orientations at the interface in which the bulky S atom remains at the aqueous side of the interface, whilst the smaller N atom, together with its smaller first hydration shell penetrates to DCE.

Finally, in interpreting the present results it should be noted that the explicit inclusion of the polarizability of the SCN^- ion in the calculation might have an important effect on its interfacial behavior. The choice of the used, pairwise additive potential model of the SCN^- ion was simply dictated by computational efficiency and by the fact that we are not aware of any existing polarizable model of this ion in the literature. Therefore, repeating the present calculations with a polarizable model for the ion seems to be an important continuation of the present study; however, this work should start with the development of a proper polarizable model. Work in this direction is currently in progress.

Acknowledgements. This work has been supported by the Hungarian OTKA Foundation under Project No. OTKA 75328, and by Fundação para a Ciência e a Tecnologia - Portugal, under Project No. PTDC/EQU-FTT/104195/2008. The authors are grateful to Dr Marcello Segal and to Prof. José A. N. F. Gomes for useful discussions. M. D. is grateful to the University of Porto for its hospitality.

References

- (1) Jarvis, N. L.; Sheiman M. A. *J. Phys. Chem.* **1968**, 72, 74.
- (2) Randles, J. E. B. *Phys. Chem. Liq.* **1977**, 7, 107.
- (3) Conway, B. E. *Adv. Coll. Int. Sci.* **1977**, 8, 91.
- (4) Hey, M. J.; Shield, D. W.; Speight, J. M.; Will, M. C. *J. Chem. Soc. Faraday Trans.* **1981**, 1, 123.
- (5) Weissenborn, P. K.; Pugh, R. J. *Langmuir* **1995**, 11, 1422.
- (6) Onsager L., Samaras, N. N. T. *J. Chem. Phys.* **1934**, 2, 528.
- (7) Wagner, C. *Phys. Z.* **1924** 25, 474.
- (8) Bhuiyan, L. B.; Bratko, D.; Outhwaite, C. W. *J. Phys. Chem.* **1991**, 95, 336.
- (9) Stairs, R. A. *Canad. J. Chem.* **1995**, 73, 781.
- (10) Karraker, K. A.; Radke C. J. *Adv. Coll. Int. Sci.* **2002**, 96, 231.
- (11) Markin, V. S.; Volkov. A. G. *J. Phys. Chem. B.* **2002**, 106, 11810.
- (12) Maheshwari, R.; Sreeram, K. J.; Dhathathreyan A. *Chem. Phys. Lett.* **2003**, 375, 157.
- (13) Manciu, M.; Ruckenstein, E. *Adv. Coll. Int. Sci.* **2003**, 105, 63.
- (14) Oshima, H.; Matsubara, H. *Colloid. Polym. Sci.* **2004**, 282, 1044.
- (15) Woelki, S.; Kohler, H. H. *Chem. Phys.* **2004**, 306, 209.
- (16) Petersen, P. B.; Johnson, J. C.; Knutsen K. P.; Saykally, R. J. *Chem. Phys. Letters* **2004**, 397, 46.
- (17) Petersen, P. B.; Saykally, R. J. *Chem. Phys. Letters* **2004**, 397, 51.
- (18) Viswanath, P.; Motschmann, H. *J. Phys. Chem. C* **2008**, 112, 2099.
- (19) Raymond, E. A.; Richmond, G. L. *J. Phys. Chem. B.* **2008**, 112, 5051.
- (20) Uchida T.; Yamaguchi, A.; Tomoni, I.; Teramae, N. *J. Phys. Chem. B* **2000**, 104, 12091.
- (21) Barker, A. L.; Unwin, P. R. *J. Phys. Chem. B* **2001**, 105, 12019.
- (22) Schröder, U.; Wadhawan, J.; Evans, R. G.; Compton, R. G.; Wood, B.; Walton, D. J.; France, R. R.; Marken, F.; Bulman Page P. C.; Hayman, C. M. *J. Phys. Chem. B* **2002**, 106, 8697.
- (23) Fujiwara, K.; Wada, S.; Monjushira, H.; Watani, H. *Langmuir* **2006**, 22, 2452.
- (24) Iwahashi, T.; Miyamae, K.; Kanai, K.; Seki, K. D.; Ouchi, Y. *Ionic Liquids: From Knowledge to Application*, ACS Symposium Series: Washington DC, **2010**.

- (25) Spohr, E. *Chem. Phys. Letters* **1993**, 207, 214.
- (26) Jungwirth, P.; Tobias, D. J. *J. Phys. Chem. B* **2002**, 106, 6361.
- (27) Dang, L. X. *J. Chem. Phys.* **2003**, 119, 9851.
- (28) Vrbka L.; Mucha M., Minofar B.; Jungwirth P.; Brown E. C.; Tobias, D. J. *Curr. Opin. Coll. Interface Sci.* **2004**, 9, 67.
- (29) Jungwirth, P.; Finlayson; B. J.; Tobias, D. J. *Chem. Rev.* **2006**, 106, 1134.
- (30) Jungwirth, P.; Tobias, D. J. *Chem. Rev.*, **2006**, 106, 1259.
- (31) Wick, C. D., Dang, L. X. *J. Phys. Chem. C* **2008**, 112, 647.
- (32) Wick, C. D., Dang, L. X. *Chem. Phys. Letters* **2008**, 458, 1.
- (33) Dang, L. X. *J. Phys. Chem. B* **1999**, 103, 8195.
- (34) Fernandes, P. A.; Cordeiro, M. N. D. S.; Gomes, J. A. N. F. *J. Phys. Chem. B* **1999**, 103, 8930.
- (35) Fernandes, P. A.; Cordeiro, M. N. D. S.; Gomes, J. A. N. F. *J. Phys. Chem. B* **2000**, 104, 2278.
- (36) Berny, F.; Schurhammer, R.; Wipff, G. *Inorg. Chim. Acta* **2000**, 300, 384.
- (37) Michael, D.; Benjamin, I. *J. Chem. Phys* **2001**, 114, 2817.
- (38) Vincze, Á.; Jedlovszky, P.; Horvai, G. *Anal. Sci.* **2001**, 17, i317.
- (39) Petersen, P. B.; Saykally, R. J. ; Mucha, M.; Jungwirth, P. *J. Phys. Chem. B.* **2005**, 109, 10915.
- (40) Winter, N.; Benjamin, I. *J. Phys. Chem. B* **2005**, 109, 16421.
- (41) Luo, G.; Malkova, S.; Yoon, J.; Schultz, D. G.; Lin, B.; Meron, M.; Benjamin, I.; Vanýsek, P.; Schlossman, M. L. *Science* **2006**, 311, 5758.
- (42) Schweighofer, K.; Benjamin, I. *J. Phys. Chem. A* **1999**, 103, 10274.
- (43) Mason, P. E.; Dempsey, C. E.; Neilson, G. W.; Brady, J. W. **J2005**, 109, 24185.
- (44) Wallace, T. P.; Stauffer, C. H. *J. Phys. Chem.* **1967**, 71, 2083.
- (45) Reeske, G.; Schürmann, M.; Costisella, B.; Jurkschat, K. *Organometallics* **2007**, 26, 4170.
- (46) Pedemonte, N.; Caci, E.; Sondo, E.; Caputo, A.; Rhoden, K.; Pfeffer, U.; Di Candia, M.; Bandettini, R.; Ravazzolo, R.; Zegarra-Moran, O.; Galiotta, L. J. *J. Immunol.* **2007**, 178, 5144.
- (47) Panzer, R.E.; Schaer M. G. *J. Electrochem. Soc.* **1965**, 112, 1136, and references therein.
- (48) Samec, Z. *Chem. Rev.* **1988**, 88, 617.
- (49) Conboy, J. C.; Richmond, G. L. *Electrochim. Acta* **1995**, 40, 2881.

- (50) Jensen, H.; Fermin, D. J.; Girault, H. H. *Phys. Chem. Chem. Phys.* **2001**, *3*, 2503.
- (51) Jones, M. A.; Bohn, P. W. *J. Phys. Chem. B* **2001**, *105*, 2197.
- (52) Walker, D. S.; Brown, M. G.; McFearn, C. L.; Richmond, G. L. *J. Phys. Chem. B* **2004**, *108*, 2111.
- (53) Walker, D. S.; Moore, F. G.; Richmond, G. L. *J. Phys. Chem. C* **2007**, *111*, 6103.
- (54) Benjamin, I. *J. Chem. Phys.* **1992**, *97*, 1432.
- (55) Schweighofer, K. J.; Benjamin, I. *J. Electroanal. Chem.* **1995**, *391*, 1.
- (56) Schweighofer, K. J.; Benjamin, I. *J. Phys. Chem.* **1995**, *99*, 9974.
- (57) Michael, D.; Benjamin, I. *J. Chem. Phys.* **1997**, *107*, 5684.
- (58) Jedlovszky, P.; Vincze, Á.; Horvai, G. *J. Chem. Phys.* **2002**, *117*, 2271.
- (59) Benjamin, I. *J. Phys. Chem. B* **2005**, *109*, 13711.
- (60) Hantal, Gy.; Darvas, M. Pártay, L. B.; Horvai, G.; Jedlovszky, P. *J. Phys.: Cond. Matter* **2010**, *22*, 284112.
- (61) Lindahl, E.; Hess, B.; van der Spoel, D. *J. Mol. Mod.* **2001**, *7*, 306.
- (62) Jorgensen, W. L.; Chandrashekar, J.; Madura, J. D.; Impey, R.; Klein, M. L. *J. Chem. Phys.* **1983**, *79*, 926.
- (63) Jorgensen, W. L.; Tirado-Rives, J. *J. Am. Chem. Soc.* **1988**, *110*, 1657.
- (64) Allen, M. P.; Tildesley, D. J. *Computer Simulation of Liquids*, Clarendon Press: Oxford, **1987**.
- (65) Miyamoto, S.; Kollman, P. A. *J. Comp. Chem.* **1992**, *13*, 952.
- (66) Hess, B.; Bekker, H.; Berendsen, H. J. C.; Fraaije, J. G. E. M. *J. Comp. Chem.* **1997**, *18*, 1463.
- (67) Essman, U.; Perera, L.; Berkowitz, M. L.; Darden, T.; Lee, H.; Pedersen, L. G. *J. Chem. Phys.* **1995**, *103*, 8577.
- (68) Berendsen, H. J. C.; Postma, J. P. M.; DiNola, A.; Haak J. R. *J. Chem. Phys.* **1984**, *81*, 3684.
- (69) Dang, L. X. *J. Phys. Chem. B* **2002**, *106*, 10388.
- (70) Pártay, L. B.; Hantal, Gy.; Jedlovszky, P.; Vincze, Á.; Horvai, G. *J. Comp. Chem.* **2008**, *29*, 945.
- (71) Onorato, R. M.; Otten, D. E.; Saykally, R. J. *Proc. Natl. Acad. Sci.* **2009**, *106*, 15176.
- (72) Pegram, L. M.; Thomas Record, M.; *Proc. Natl. Acad. Sci.* **2006**, *103*, 14278.
- (73) Osakai, T.; Ogata, A.; Ebina, K. *J. Phys. Chem. B* **1997**, *101*, 8341.

Tables

TABLE 1: Interaction Parameters of the Molecular Models Used

Molecule	Interaction site	σ (Å)	ϵ (kJ mol ⁻¹)	q (e)
Water ^a	O _w	3.154	0.649	0.000
	H _w	0.000	0.000	0.520
	M _w ^b	0.000	0.000	-1.040
SCN ^c	S	3.550	1.046	-0.75
	C	3.750	0.439	0.49
	N	3.250	0.711	-0.74
DCE ^d	CH ₂	3.800	0.494	0.227
	Cl	3.400	1.255	-0.227

^aTIP4P model, ref. 62.

^bNon-atomic interaction site, placed along the H-O-H bisector 0.15 Å away from the O atom toward the hydrogens.

^cOPLS model, ref. 63.

^dLennard-Jones parameters correspond to the OPLS model, ref. 64, fractional charges are taken from ref. 54.

TABLE 2: Geometry Parameters of the Molecular Models Used in the Simulations

Molecule	Bond	Length (Å)	Bond angle	Angle (deg)
Water ^a	O-H	0.9572	H-O-H	104.52
SCN ^b	S-C	1.670	S-C-N	180
	C-N	1.190		
DCE ^c	CH ₂ -CH ₂	1.53	Cl-CH ₂ -CH ₂	108.2
	CH ₂ -Cl	1.79		

TABLE 3: Partial First Shell Hydration Numbers Corresponding to the Different Atoms of the SCN^- Ion, n_{hyd} , and Molecular Hydration Numbers, N_{hyd} , Obtained as the Sum of the Contributions of the S and N Atoms

Ion Position	Atom pairs	n_{hyd}	N_{hyd}
Bulk water	$\text{O}_w - \text{S}$	2.3	3.9
	$\text{O}_w - \text{C}$	4.3	
	$\text{O}_w - \text{N}$	1.6	
Subsurface water	$\text{O}_w - \text{S}$	2.3	4.3
	$\text{O}_w - \text{C}$	3.9	
	$\text{O}_w - \text{N}$	2.0	
Interface water	$\text{O}_w - \text{S}$	1.9	3.8
	$\text{O}_w - \text{C}$	3.3	
	$\text{O}_w - \text{N}$	1.9	
Interface DCE	$\text{O}_w - \text{S}$	1.8	3.5
	$\text{O}_w - \text{C}$	3.0	
	$\text{O}_w - \text{N}$	1.7	
Subsurface DCE	$\text{O}_w - \text{S}$	2.0	3.8
	$\text{O}_w - \text{C}$	3.1	
	$\text{O}_w - \text{N}$	1.8	
Bulk DCE	$\text{O}_w - \text{S}$	2.2	4.2
	$\text{O}_w - \text{C}$	4.0	
	$\text{O}_w - \text{N}$	2.0	

Figure legend

Figure 1. Solvation free energy profile of the SCN^- ion across the water/DCE interface (top panel). Error bars estimated by the method of block averages are also shown. For reference, the mass density profiles of the water (open circles) and DCE molecules (filled circles), obtained in the ion free system⁶⁰ are also shown (bottom panel). The dashed vertical lines show the division of the system into six separate regions (see the text). The inset shows the local minimum of the free energy profile at the subsurface water region on a magnified scale.

Figure 2. Partial pair correlation functions of the S (solid lines), C (dashed lines) and N atom (dash-dot-dotted lines) of the SCN^- ion and the water oxygens, as obtained in the bulk water (top panel), interfacial water (second panel), interfacial DCE (third panel), and bulk DCE (bottom panel) regions of the system.

Figure 3. Total hydration number of the SCN^- ion, estimated as the sum of the partial hydration numbers of the S and N atoms (see the text) in the six separate regions of the system. The black and white portions of the bars represent the contributions of the partial hydration number of the S and N atoms, respectively, to the estimated total hydration number.

Figure 4. Chart illustrating the definition of the angle γ characterizing the interfacial orientation of the SCN^- ion (top); and cosine distribution of the angle γ as obtained in the six different regions of the system (bottom). The results corresponding to the bulk water (solid line), subsurface water (dashed line), interfacial water (dotted line), interfacial DCE (dash-dotted line), subsurface DCE (dash-dot-dotted line), and bulk DCE (short dashed line) regions of the system are shifted by 0.5, 0.4, 0.3, 0.2, 0.1 and 0 units, respectively, for clarity.

Figure 5. Two instantaneous snapshots, taken out from the simulations, illustrating the interfacial orientation of the SCN^- ion and the co-extraction of its first hydration shell upon entering to the organic phase. Water molecules are shown by grey color; the S, C and N atoms of the SCN^- ion are represented by a yellow, light blue and dark blue sphere, respectively. DCE molecules are omitted from the figure for clarity.

Figure 1.
Darvas et al.

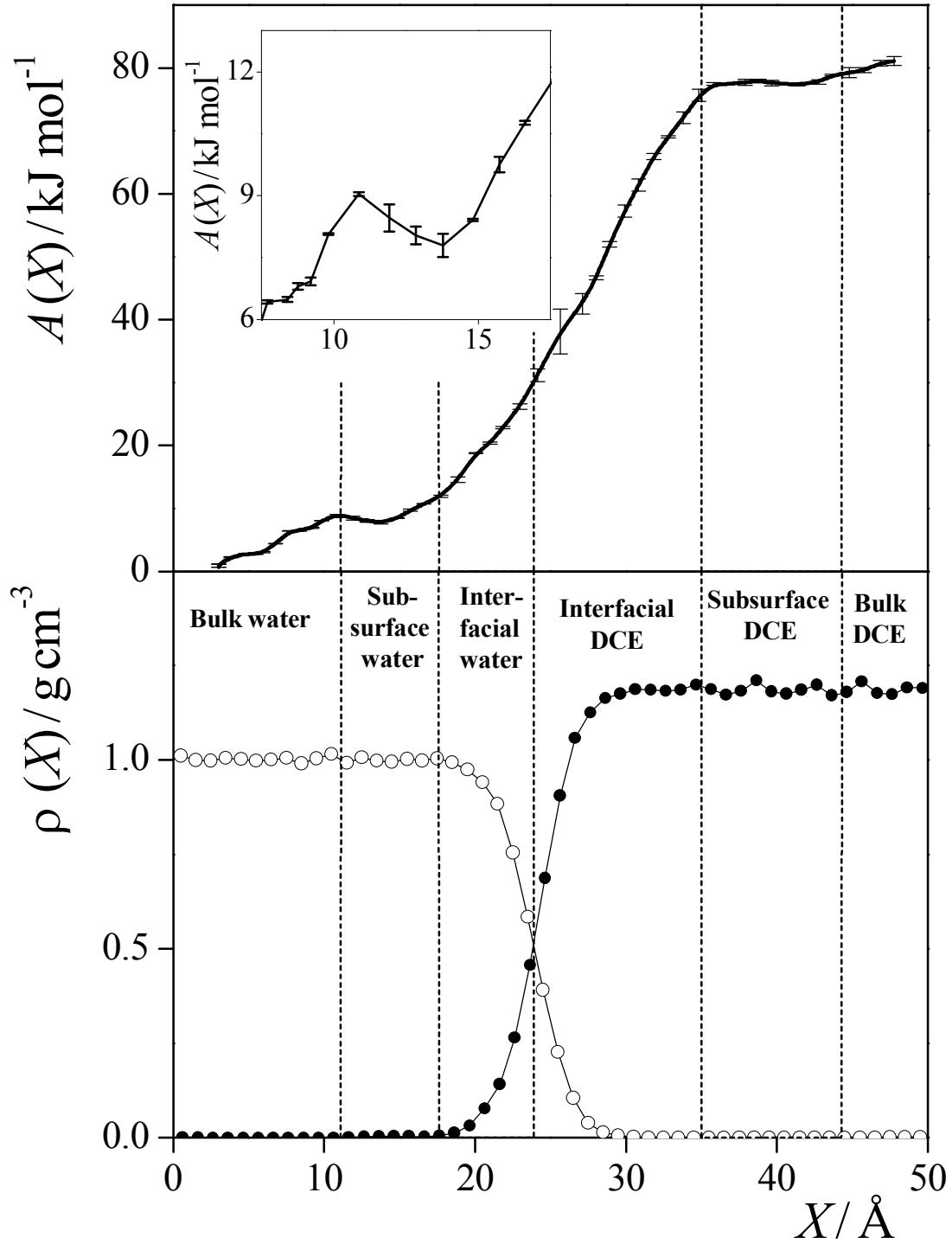


Figure 2.
Darvas et al.

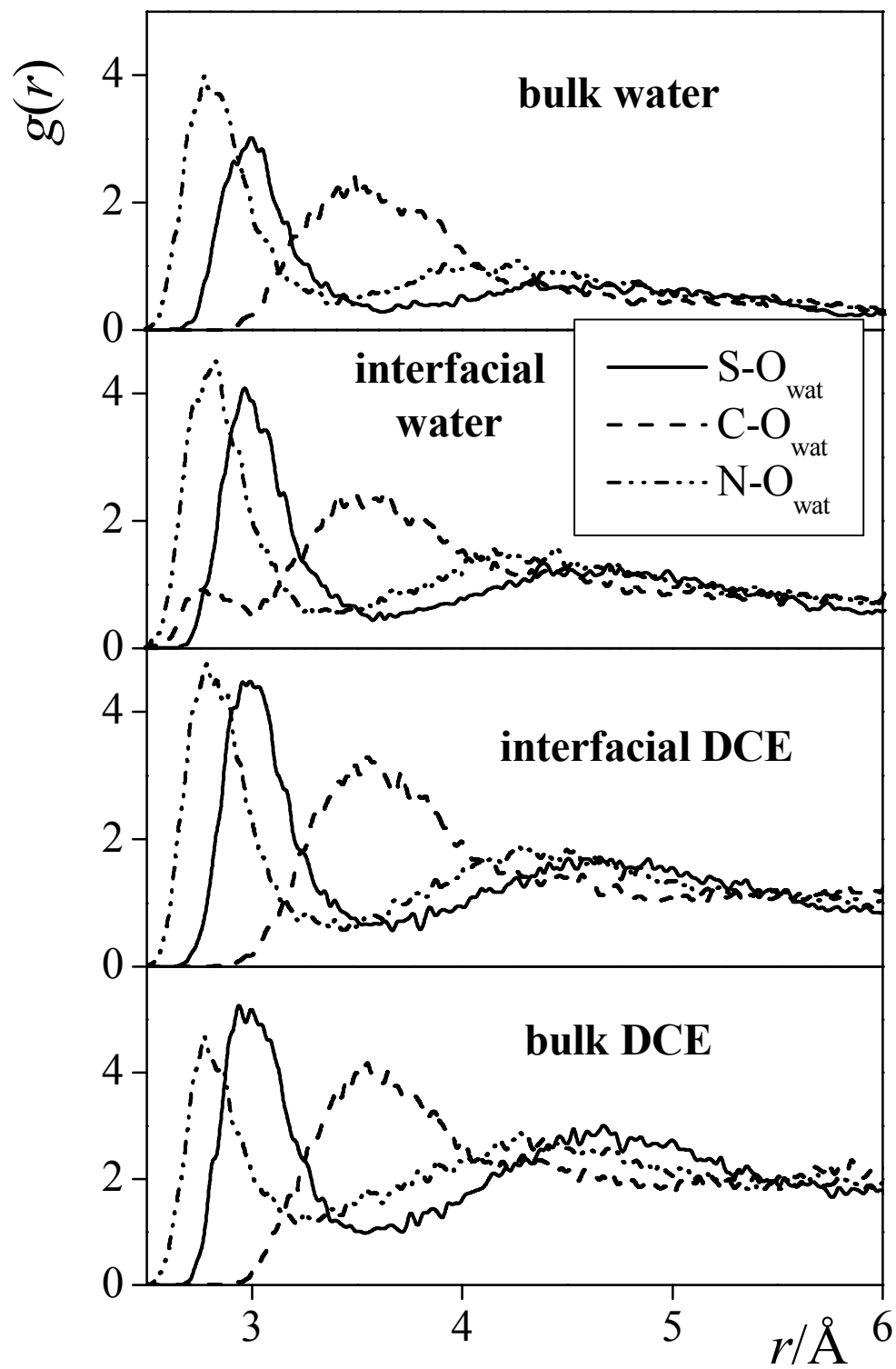


Figure 3.
Darvas et al.

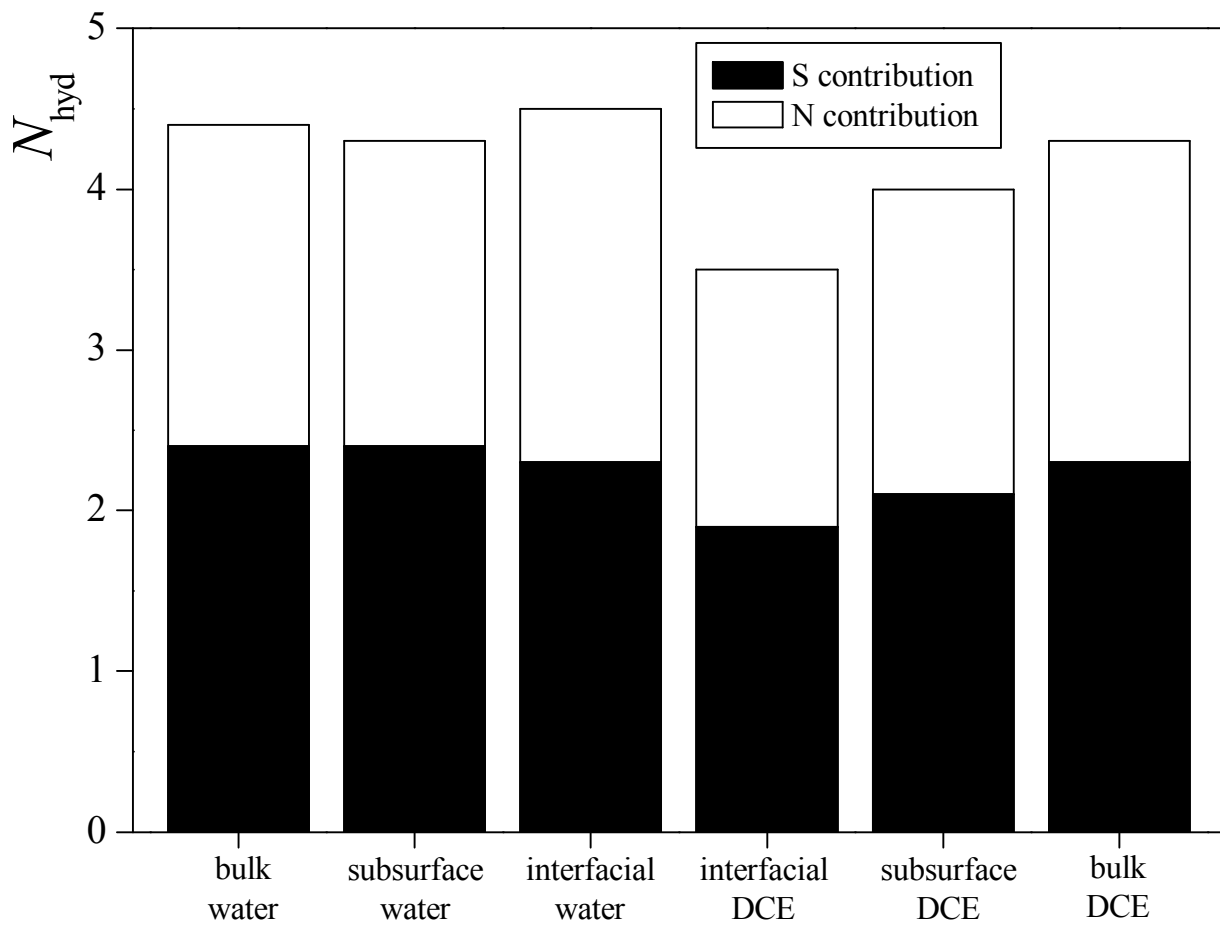


Figure 4.
Darvas et al.

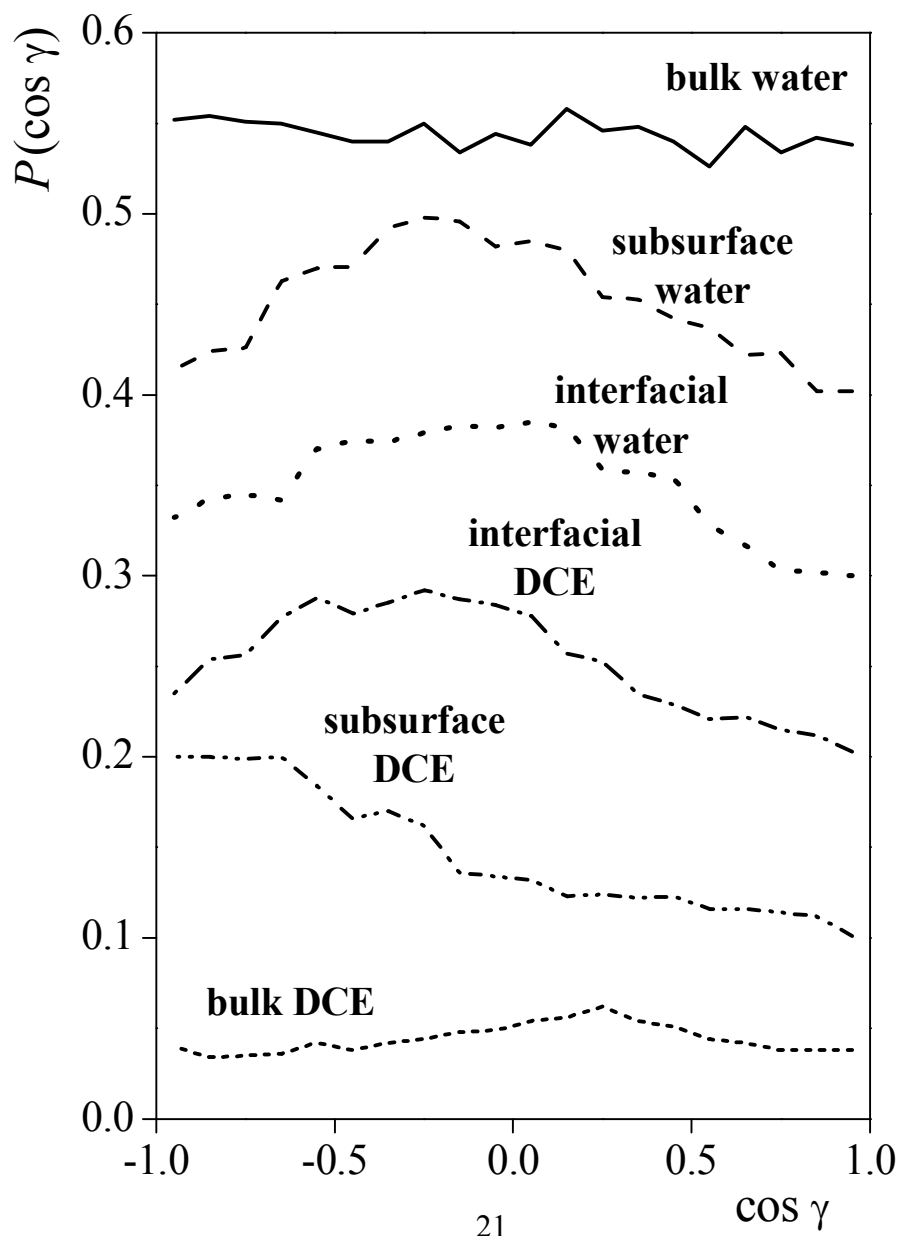
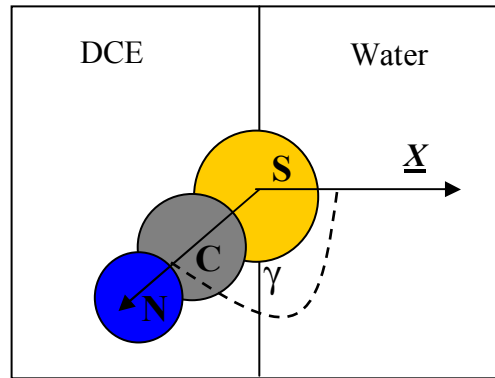


Figure 5.
Darvas et al.

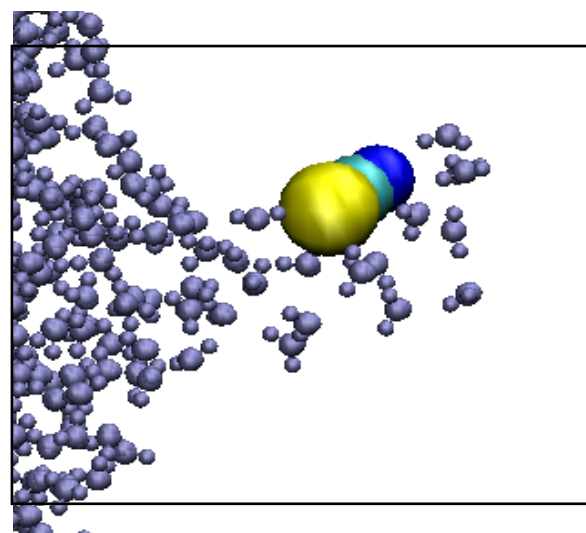
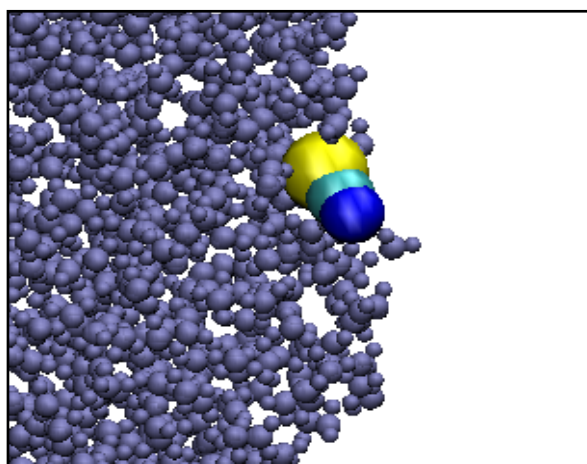


Table of Contents Graphics:

